

Symmetrical Intersections of Cylinders

BY IAN O. ANGELL

Department of Information Systems, London School of Economics, Houghton Street,
London WC2A 2AE, England

AND MORETON MOORE

Department of Physics, Royal Holloway and Bedford New College, Egham, Surrey TW20 0EX, England

(Received 11 April 1986; accepted 23 September 1986)

Abstract

There are four regular cylindrical solids, comprising the symmetrical intersections of three, four, six and ten cylinders of equal radius; two quasi-regular solids, six and 15; and their duals, seven and 16 cylinders respectively. There are further solids with cubic crystal symmetry formed by the intersection of six, 12 or 24 cylinders with axes along $\langle hkl \rangle$ directions; as well as combinations of forms. Their volumes are independent of π and are equal to $\frac{1}{3} \times$ surface area \times radius. Possible applications to the geometry of laser fusion and to crystal dissolution morphology are briefly considered.

1. Introduction

Intersections of two cylinders are found in a variety of situations: where pipes of circular cross section meet or where the barrel vaulting of Norman or Romanesque architecture intersects in a cross vault. Here larger numbers of intersecting equi-radial cylinders are considered, which display cubic crystal symmetry. The crystallographic axes available and the resulting shapes are discussed in § 2. An alternative description of symmetric axes is given in § 3, by considering the body diagonals of regular and less-regular solids. The surface areas and volumes of the solids are derived in § 4, and models and possible applications are considered in §§ 5 and 6.

2. Crystallographic axes and resulting shapes

2.1. Systems of axes with cubic crystal symmetry

Consider zone axes of crystals with cubic symmetry. In Table 1 the zone-axis symbols $\langle hkl \rangle$ are listed in order of increasing $N = h^2 + k^2 + l^2$. For example, there are three $\langle 100 \rangle$ axes: [100], [010] and [001]. $\langle 200 \rangle$ axes are equivalent to $\langle 100 \rangle$, and so on. For $\langle 210 \rangle$ axes, an example of $h \neq k$ and $l = 0$, one may take all 12 permutations, or just the six which preserve the cyclic order of 2, 1 and 0. (The anti-cyclic order will give the same solid formed by intersecting cylinders, but in the opposite setting.) The same is true

Table 1. Solids formed by intersecting cylinders arranged by zone axes

<i>N</i>	<i>hkl</i>	Cyclic	Permutations	Figure no.
1	100		3	2
2	110		6	4
3	111		4	3
4	200 = 100			
5	210	6	12	7, 10
6	211		12	12
7	—		—	
8	220 = 110			
9	221		12	14
9	300 = 100			
10	310	6	12	6, 9
11	311		12	13
12	222 = 111			
13	320	6	12	8, 11
14	321	12	24	15, 16
15	—		—	
16	400 = 100			

for $\langle 310 \rangle$ and $\langle 320 \rangle$ axes. For $\langle 211 \rangle$, $\langle 221 \rangle$ and $\langle 311 \rangle$, in which two indices are the same and no index is zero, there are 12 permutations. For non-zero indices which are all different, e.g. $\langle 321 \rangle$, there are 12 cyclic permutations, and 24 if all permutations are allowed.

In Table 1, gaps occur for those numbers *N* which cannot be expressed as the sum of three squares: 7, 15, 23, 28, 31, ..., $4^m(8n+7)$, where *m* and *n* are positive integers or zero (Davenport, 1968). [The alternative expression $p^2(8q-1)$, in which *p* and *q* are positive integers, generates the same set of numbers.] The table may of course be extended.

24 is the largest number of identical axes displaying cubic crystal symmetry (since the order of the holosymmetric cubic class is 48). Certain larger numbers may of course be achieved by combining several different systems of axes, the numbers being additions (or multiples) of 6, 12 or 24, together with the possibility of the single addition of 3 or 4, or both (i.e. 7).

2.2. Cylindrical solids with cubic crystal symmetry

The minimum number of intersecting cylinders needed for cubic symmetry is three and their axes, lying along the $\langle 100 \rangle$ directions, are mutually orthogonal. Fig. 1 shows a perspective view of the resulting shape. Here the axes of the three cylinders are represented by chain-dotted lines and the outlines

of two of the cylinders have been drawn. The horizontal straight lines which shade two of the facets of the intersection solid are generators of one of the cylinders. Two more facets, at the rear of the diagram, belong to this cylinder. There are 12 cylindrical facets in all, and if tangent planes were constructed touching them in the generators joining the threefold vertices, a rhombic dodecahedron would result. Fig. 2 shows orthographic projections, drawn by computer, along the [100], [110], [111] and [321] directions.

There are four $\langle 111 \rangle$ directions, and taking these as axes for intersecting cylinders, the solid of 24 facets depicted in Fig. 3 results. The solid formed by the six $\langle 110 \rangle$ axes is shown in Fig. 4. Note the circular cross sections in the [100], [111] and [110] projections of Figs. 2, 3 and 4 respectively, and the relatively sharp vertices of the other views, especially in Figs. 2 and 3 where the vertices protrude to a distance $(3/2)^{1/2}$ ($=1.225$) from the centre relative to cylinders of unit radius. Fig. 5 shows the intersection solid

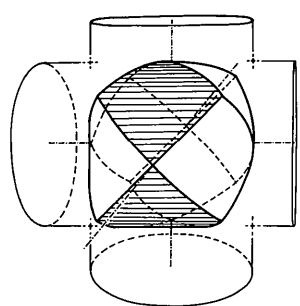


Fig. 1. Perspective view of the solid common to three equi-radial cylinders, whose axes are mutually orthogonal.

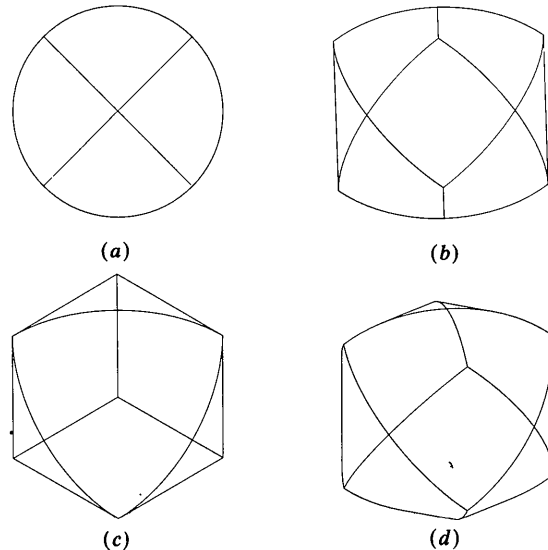


Fig. 2. The intersection of three equal $\langle 100 \rangle$ cylinders whose axes join the opposite vertices of an octahedron. Views along (a) [100], (b) [110], (c) [111] and (d) [321].

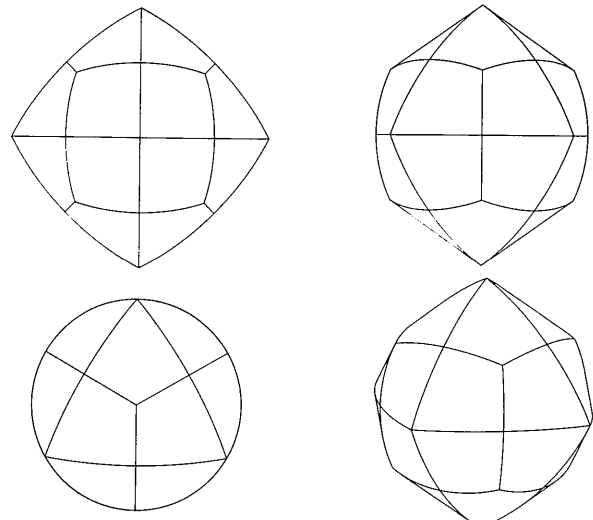


Fig. 3. Four $\langle 111 \rangle$ cylinders: axes joining opposite vertices of a cube.

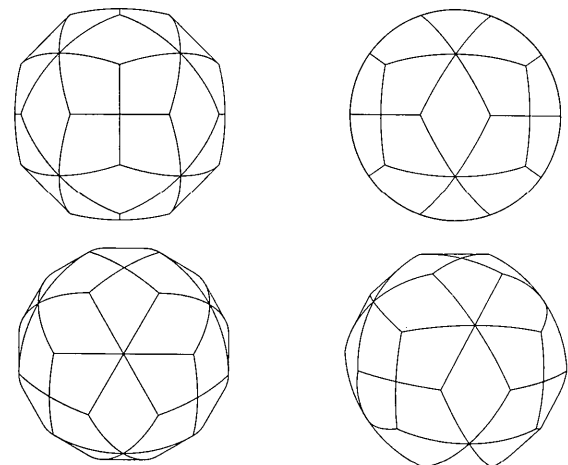


Fig. 4. Six $\langle 110 \rangle$ cylinders: axes joining opposite vertices of a cuboctahedron.

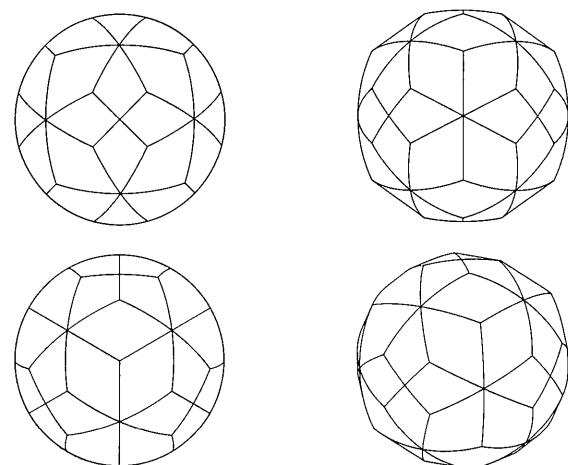


Fig. 5. Seven $\langle 100 \rangle + \langle 111 \rangle$ cylinders: joining opposite vertices of a rhombic dodecahedron.

formed by seven cylinders: three $\langle 100 \rangle$ and four $\langle 111 \rangle$. It is thus a combination of forms and the figure clearly shows the circular cross sections looking along $[100]$ and $[111]$.

Other combinations of six cylinders are shown in Figs. 6, 7 and 8. These show the solids formed by the cyclic permutations of $\langle 310 \rangle$, $\langle 210 \rangle$ and $\langle 320 \rangle$ in the progression of k/h from $\frac{1}{3}$ through $\frac{1}{2}$ to $\frac{2}{3}$. The progression may be seen in the solids. The solid of Fig. 17 (discussed later) with pentad symmetry belongs in this series with $k/h = 0.618$. The corresponding

complete permutations of $\langle 310 \rangle$, $\langle 210 \rangle$ and $\langle 320 \rangle$ are shown in Figs. 9, 10 and 11 respectively.

There are certain similarities amongst Figs. 12 $\langle 211 \rangle$, 13 $\langle 311 \rangle$ and 14 $\langle 221 \rangle$, in each of which two indices are the same. The most general case, with all indices different and non-zero, exemplified by $\langle 321 \rangle$, is shown for cyclic permutations in Fig. 15 and for all permutations in Fig. 16: 12 and 24 cylinders respectively. The surface of the latter is divided into 48 'triangular' regions each containing 19 facets, giving a total of 912 in all.

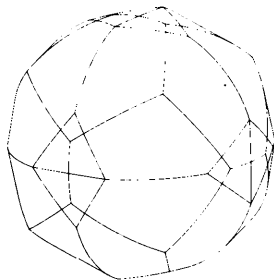


Fig. 6. Six cylinders: $\langle 310 \rangle$ cyclic permutations. View along [321].

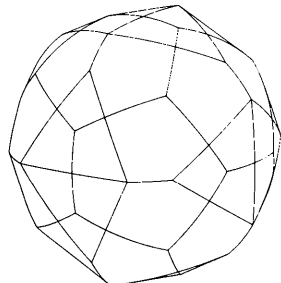


Fig. 7. Six cylinders: $\langle 210 \rangle$ cyclic.

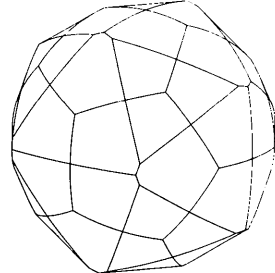


Fig. 8. Six cylinders: $\langle 320 \rangle$ cyclic.

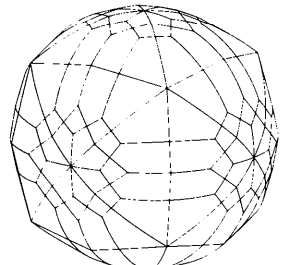


Fig. 9. 12 cylinders: $\langle 310 \rangle$ all permutations.

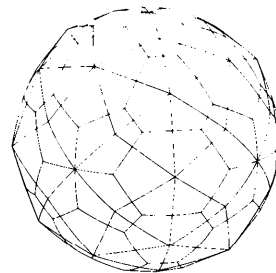


Fig. 10. 12 cylinders: $\langle 210 \rangle$ all permutations.

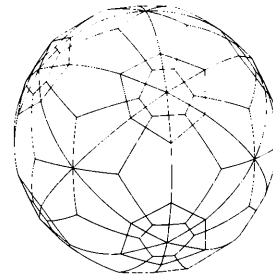


Fig. 11. 12 cylinders: $\langle 320 \rangle$ all permutations.

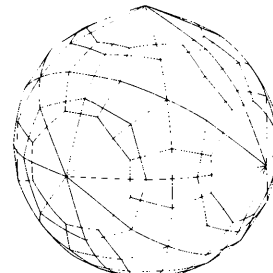


Fig. 12. 12 cylinders: $\langle 211 \rangle$.

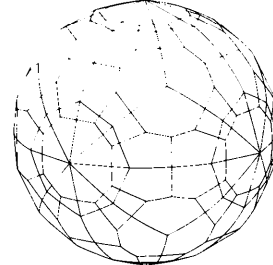


Fig. 13. 12 cylinders: $\langle 311 \rangle$.

The shapes derived from cyclic permutations of $\langle hkl \rangle$, $h \neq k \neq l$, possess only $(2/m)\bar{3}$ symmetry; whilst for all permutations, holosymmetric $(4/m)\bar{3}(2/m)$ morphologies result.

3. Regular and quasi-regular solids

As an alternative description for symmetric axes, the body diagonals of the various regular and less-regular solids may be considered. There are five regular convex (Platonic) solids, with the property that all faces are equivalent and so also are all the vertices. Of these the cube and octahedron have already been considered: the body diagonals of the octahedron are the three $\langle 100 \rangle$ directions (the cylindrical solid is shown in Fig. 2), and the body diagonals of the cube are the four $\langle 111 \rangle$ directions (Fig. 3). The tetrahedron is non-centrosymmetric and in any case the joins from the centre to its four vertices give the same four $\langle 111 \rangle$ directions as for the cube. The icosahedron, which

has 12 vertices, gives rise to six cylinder axes, whilst the (pentagonal) dodecahedron of 20 vertices gives a solid formed from ten cylinders. These are shown in Figs. 17 and 18 respectively. [The non-convex regular (Kepler-Poinsot) polyhedra also have these body diagonals.] Thus there are four regular cylindrical solids.

There are several classes of less-regular solids. [For a discussion of these see Fejes Tóth (1964).] The Archimedean solids have equivalent vertices but differing regular polygonal faces. Their duals (the Catalan solids) have equivalent faces but differing vertices. For example, the cuboctahedron has 12 vertices, six square faces and eight triangular ones. Its dual, the rhombic dodecahedron, has 12 rhombic faces, six fourfold vertices and eight threefold ones.

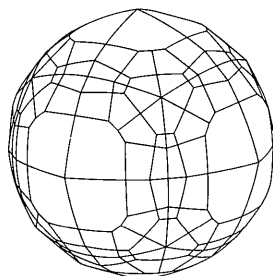


Fig. 14. 12 cylinders: $\langle 221 \rangle$.

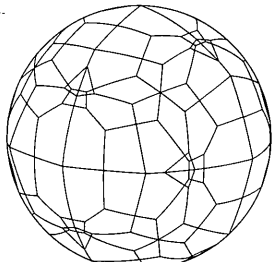


Fig. 15. 12 cylinders: $\langle 321 \rangle$ cyclic permutations.

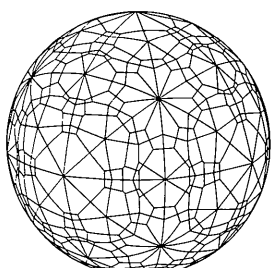


Fig. 16. 24 cylinders: $\langle 321 \rangle$ all permutations.

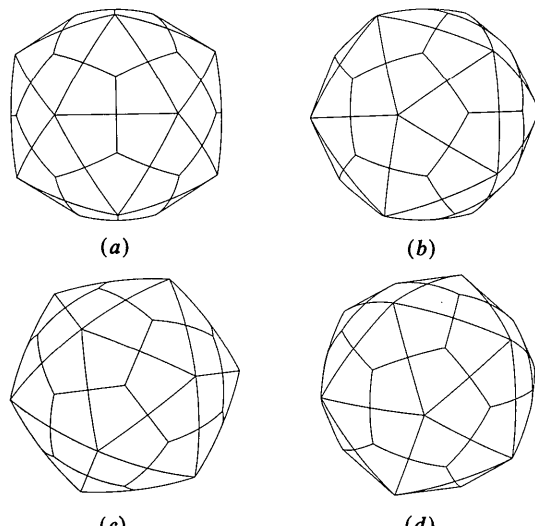


Fig. 17. Six cylinders: axes joining opposite vertices of an icosahedron. Views along (a) $\langle 100 \rangle$, (b) $\langle 110 \rangle$, (c) $\langle 111 \rangle$ and (d) $\langle 321 \rangle$.

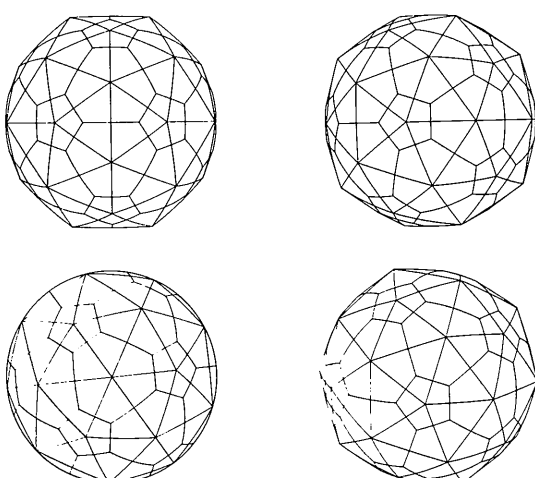


Fig. 18. Ten cylinders: axes joining opposite vertices of a (pentagonal) dodecahedron.

(Both solids have 24 edges.) The diagonals of the cuboctahedron are the six $\langle 110 \rangle$ directions; the cylindrical solid derived from these has already been considered and is shown in Fig. 4. The body diagonals of the rhombic dodecahedron comprise the three $\langle 100 \rangle$ and four $\langle 111 \rangle$ directions: the combination of forms whose cylindrical solid is shown in Fig. 5.

The cuboctahedron is a combination of cube and octahedron, and in a similar manner the icosidodecahedron is a combination of icosahedron and dodecahedron. It has 30 vertices and the corresponding cylindrical solid of 15 axes is shown in Fig. 19. The dual of the icosidodecahedron is the rhombic triacontahedron. This has $(12+20=) 32$ vertices and the solid of 16 cylinders is shown in Fig. 20. From the Archimedean solids, Fejes Tóth (1964) selects those with equivalent edges, the cuboctahedron and icosidodecahedron, and calls them quasi-regular. Robertson & Carter (1970) have also noted their importance. The regular and quasi-regular solids with the numbers of their body diagonals are listed in Table 2, arranged as pairs of dual solids.

Polyhedra listed in column A each have six diads, four triads and three tetrad axes of rotational symmetry, and also nine mirror planes (*i.e.* they have full cubic symmetry in the crystallographic sense). Those in column B have 15 diads, ten triads, six pentads and 15 mirror planes (*i.e.* full icosahedral symmetry). Such symmetries are also exhibited by the solids formed by intersecting cylinders whose axes are the body diagonals of these polyhedra.

For solids of group A (those with tetrad axes of symmetry) the cylinder axes are as follows: Fig. 2 three axes: $\langle 100 \rangle$; Fig. 3 four axes: $\langle 111 \rangle$; Fig. 4 six axes: $\langle 110 \rangle$; Fig. 5 seven axes: $\langle 100 \rangle + \langle 111 \rangle$.

For solids of group B (with pentad axes) the 'golden ratio' τ is required. It satisfies the quadratic equation $\tau^2 - \tau - 1 = 0$, and takes the value $(1 + \sqrt{5})/2 \approx 1.61803$. Fig. 17 six axes: cyclic permutations

Table 2. *Regular and quasi-regular solids arranged as pairs of duals*

	A	B
Regular	Octahedron: 3 Cube: 4	Icosahedron: 6 Dodecahedron: 10
Quasi-regular	Cuboctahedron: 6 Rhombic dodecahedron: 7	Icosidodecahedron: 15 Rhombic triacontahedron: 16

of $\langle \tau 10 \rangle$; Fig. 18 ten axes: $\langle 111 \rangle +$ cyclic permutations of $\langle \tau -1 \tau 0 \rangle$; Fig. 19 15 axes: $\langle 100 \rangle +$ cyclic permutations of $\langle \tau \tau +1 1 \rangle$; Fig. 20 16 axes: those of Figs. 17 and 18 together. Fig. 17 belongs in the series (Figs. 6, 7 and 8) of cyclic permutations of $\langle hk0 \rangle$ discussed above.

One could continue the discussion with all the Archimedean solids and their duals, and the infinite classes of prisms and anti-prisms. Suffice it to say that a good number of Archimedean solids have already been considered in § 2.2. The joins from the centre to the vertices of the truncated tetrahedron are the twelve $\langle 311 \rangle$ directions and the corresponding cylindrical solid is shown in Fig. 13. The body diagonals of the truncated octahedron are the 12 $\langle 210 \rangle$ directions: see Fig. 10. The truncated cube (with regular octagonal faces) has 12 body diagonals $\langle h11 \rangle$ and the diagonals of the rhombicuboctahedron are the 12 $\langle hh1 \rangle$ directions, where $h = \sqrt{2} - 1$ (≈ 0.414) in each case. The great rhombicuboctahedron (or truncated cuboctahedron), with regular octagonal and hexagonal as well as square faces, has 24 body diagonals of $\langle hk1 \rangle$ type, where $h = 1 + 2\sqrt{2}$ and $k = 1 + \sqrt{2}$: again irrational indices.

4. Volumes of the solids

The volumes of these solids, expressed in terms of their radius R (or diameter D) do not contain π ! The intersection of two equal cylinders at right angles

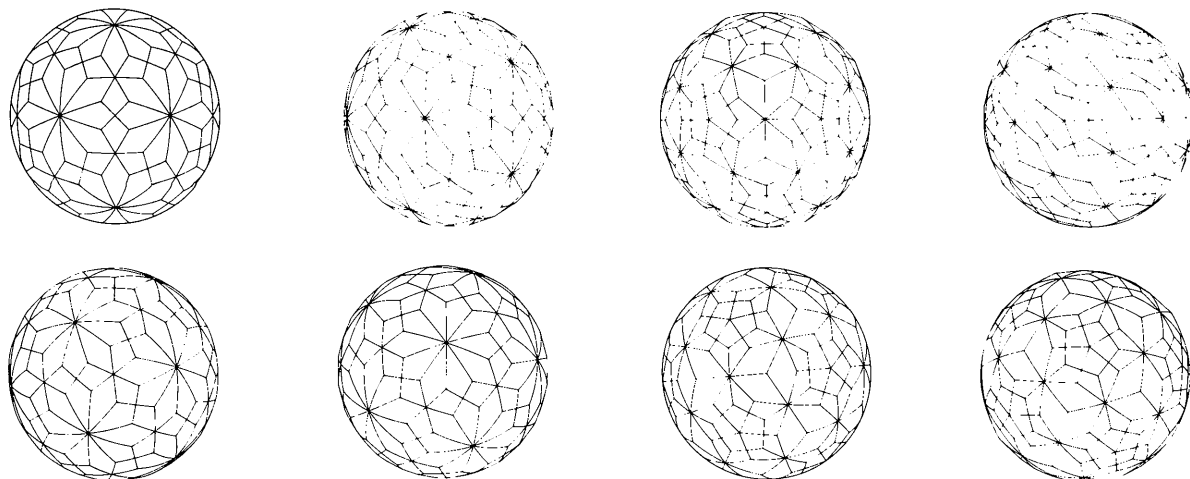


Fig. 19. 15 cylinders: derived from the icosidodecahedron.

Fig. 20. 16 cylinders: derived from the rhombic triacontahedron.

was known to Archimedes (ca. 250 BC; see also Gardner, 1962), who considered the circles inscribed within the square sections of the solid. The areas of the squares ($4r^2$) are larger than those of the circles (πr^2) by the constant ratio $4/\pi$; and as the circles enclose a sphere of volume $4\pi R^3/3$, the volume of the solid common to both cylinders is larger than this by the same factor: $(4/\pi) \times 4\pi R^3/3 = 16R^3/3 = 2D^3/3$: a strangely simple result.

Hubbell (1965) has considered the general case of the volume common to two cylinders of different radii intersecting at the arbitrary angle β , a much more complicated situation with the volume involving either hypergeometric series or elliptic integrals. For equal radii, however, the volume is simply $16R^3/(3 \sin \beta)$.

The volume of the symmetrical solid common to three $\langle 100 \rangle$ cylinders lacks a factor of π (Moore, 1973), and this is also true for the solids formed by four $\langle 111 \rangle$ and by six $\langle 110 \rangle$ intersecting cylinders (Moore, 1974). This apparently surprising result may be explained by considering each solid as being made up of a number of cylindrical sectors with vertices $O (0, 0, 0)$, $A (R, 0, 0)$, $B (R, \theta, 0)$, $C (R, \theta, Z)$, expressed in cylindrical polar coordinates: see Fig. 21. Each cylindrical facet of the solid may be divided into several cylindrical triangles such as ABC : AB is a circular arc of radius R in the plane OAB perpendicular to the axis of the cylinder, BC is a straight line parallel to this axis (i.e. it is part of a generator of the cylinder), and COA is a plane intersecting the cylindrical surface in the elliptical arc CA .

The height h of the elementary strip XY compared with that of BC is $h/Z = (R \sin \theta)/(R \sin \Theta)$, where θ is the angle XOA and Θ the angle BOA ; giving $h = Z(\sin \theta / \sin \Theta)$. The area A of the surface ABC is

$$\int_0^\Theta h(R d\theta) = (RZ / \sin \Theta)(1 - \cos \Theta) \\ = RZ(\cosec \Theta - \cot \Theta).$$

The volume V of $OABC = \int_0^\Theta \frac{1}{3}Rh(R d\theta) = AR/3$.

The result $V = AR/3$, true for cylindrical sectors as well as for complete cylindrical solids, relies on the fundamental formula for the volume of a pyramid

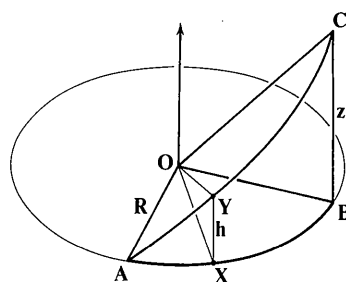


Fig. 21. Cylindrical triangle ABC .

or cone being $\frac{1}{3} \times \text{base area} \times \text{height}$. This is related to Gauss's theorem for the position vector \mathbf{r} , since $\text{div } \mathbf{r} = 3$ and $\iiint \text{div } \mathbf{r} dV = 3V = \iiint \mathbf{r} \cdot d\mathbf{S} = \text{base area} \times \text{height}$. In the limiting case of infinitely many cylinders intersecting in a sphere, the volume is $(4\pi R^2)R/3$: the familiar $\frac{4}{3}\pi R^3$.

For the example of the solid common to the three $\langle 100 \rangle$ cylinders, each of the 12 rhombic facets may be divided into four equal cylindrical triangles, one of which has vertices $(R, 0, 0)$, $(R, \pi/4, 0)$ and $(R, \pi/4, R/2)$. Thus in the formula $\Theta = \pi/4$, $Z = R/\sqrt{2}$, and the total volume is

$$(12 \times 4 \times \frac{1}{3}R^2)(\sqrt{2} - 1)R/\sqrt{2} = D^3(2 - \sqrt{2}).$$

In the same way, $V(111) = (3/\sqrt{2})(2 - \sqrt{3})D^3$ and $V(110) = \frac{2}{3}(3 + 2\sqrt{3} - 4\sqrt{2})D^3$, since the kite-shaped facets may also be subdivided into cylindrical triangles of the required form. Expressed in decimals the volumes are $0.586D^3$, $0.568D^3$ and $0.538D^3$ respectively. As the number of intersecting cylinders increases, the volumes of the solids thus formed quickly converge to the volume of a sphere, $\pi D^3/6 = 0.524D^3$.

5. Models

Complete cylindrical surfaces are easy to make by lathe. Machining accuracy, however, has to be great if a good result is to be obtained for the shape common to several intersecting cylinders. For example, if the perpendicular axes of two cylinders of 1 cm radius do not intersect in a mathematical point but miss one another by 0.001 cm, the error at the surface is a noticeable 0.1 cm.

The chord y cut off from the surface of the first cylinder by the second, and the separation x of the axes, are related by the semi-angle θ subtended at the centre: see Fig. 22 and Table 3.

$$x = 1 - \cos \theta, \\ y = 2 \sin \theta = 2[x(2-x)]^{1/2}.$$

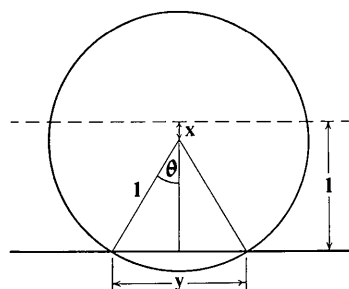


Fig. 22. The amount y cut off from a cylinder of unit radius by another at right angles. x measures the distance between the axes of the cylinders.

Table 3. Relationship between x and y for cylinders of unit radius

x	0	0.000001	0.00001	0.0001	0.001	0.01	0.1	1
y	0	0.003	0.009	0.03	0.1	0.3	0.9	2

6. Applications

6.1. The geometry of laser fusion

When apparatus is designed for laser fusion, consideration is given to arranging several pairs of inward-pointing lasers so that the axes of their beams intersect at a point. If the laser beams are assumed to have circular cross sections, the volume illuminated by all the lasers will be the intersection of right circular cylinders. For reasons of thermal stability of the excited plasma at the centre, the lasers are usually arranged in a symmetrical fashion. Here various possible arrangements have been considered.

6.2. Dissolution of cubic crystals

The morphologies of partially dissolved crystals are frequently rounded (Heimann, 1975), but edges and vertices may still be well defined. A dissolution shape depends on the starting conditions and continuously changes as dissolution proceeds (Frank, 1972). Even if the chamfering of edges may be approximated by parts of cylindrical surfaces, which eventually join with others from parallel edges to form completed cylinders, it would be unusual for a dissolving crystal if the axes of such cylinders passed through a single point. The edges grouped around a given symmetry axis of a dissolved crystal often fail to meet on the axis as they should in an ideally symmetric body; and in etching experiments surface roughening and etch pitting often mask any underly-

ing ideal morphology. Notwithstanding these misgivings, there are rare occasions when some of the solids depicted here resemble actual dissolution bodies. For example, Fig. 2 bears a similarity to dissolved crystals of the diamond structure [Ellis, 1954; Batterman, 1957 (see Fig. 11, p. 1239); Moore & Lang, 1974].

7. Concluding remarks

All the regular and quasi-regular solids for intersecting cylinders have been drawn, we believe for the first time. They may have relevance in certain applications, but in any case they have a beauty of their own.

We thank Professor Sir Charles Frank FRS and the referees for their constructive comments during the preparation of this manuscript.

References

ARCHIMEDES (ca. 250 BC). *The Method*. English translation by T. L. HEATH (1912). Reprinted 1953. New York: Dover.
 BATTERMAN, B. W. (1957). *J. Appl. Phys.* **28**, 1236-1241.
 DAVENPORT, H. (1968). *The Higher Arithmetic*, p. 126. London: Hutchinson.
 ELLIS, R. C. (1954). *J. Appl. Phys.* **25**, 1497-1499.
 FEJES TÓTH, L. (1964). *Regular Figures*, ch. IV. Oxford: Pergamon.
 FRANK, F. C. (1972). *Z. Phys. Chem. (Frankfurt am Main)*, **77**, 84-92.
 GARDNER, M. (1962). *Sci. Am.* **207**(5), 164.
 HEIMANN, R. B. (1975). *Auflösung von Kristallen*. Vienna: Springer.
 HUBBELL, J. H. (1965). *J. Res. Natl Bur. Stand. Sect. C*, **69**(2), 139-143.
 MOORE, M. (1973). PhD thesis, Univ. of Bristol, Vol. 1, p. 17.
 MOORE, M. (1974). *Math. Gaz.* **58**, 181-185.
 MOORE, M. & LANG, A. R. (1974). *J. Cryst. Growth*, **26**, 133-139.
 ROBERTSON, S. A. & CARTER, S. (1970). *J. London Math. Soc.* (2), **2**, 125-132.

Treatment of Enhanced Zones and Rows in Normalizing Intensities

BY A. J. C. WILSON

Crystallographic Data Centre, University Chemical Laboratory, Lensfield Road, Cambridge CB2 1EW, England

(Received 11 July 1986; accepted 1 October 1986)

Abstract

Contrary to the recommendation in some textbooks, enhanced reflexions should not be divided by the enhancement factor in forming general averages for normalization. The intensity required for the enhancement is drawn from the adjacent reflexions

in the reciprocal lattice, and the correct average intensity is obtained by including all reflexions at their observed intensity. Weights based on the *number* of reflexions of different types intercepted by the spherical shell that defines those included in the average may be appropriate.